IV.C.1p Multiply Surface-Functionalized Nanoporous Carbon for Vehicular Hydrogen Storage

P. Pfeifer (Primary Contact), C. Wexler, G. Suppes, F. Hawthorne, S. Jalisatgi, M. Lee, D. Robertson
University of Missouri
223 Physics Building
Columbia, MO 65211
Phone: (573) 882-2335; Fax: (573) 882-4195
E-mail: pfeiferp@missouri.edu

DOE Technology Development Manager: Carole Read
Phone: (202) 586-3152; Fax: (202) 586-9811
E-mail: Carole.Read@ee.doe.gov

DOE Project Officer: Jesse Adams
Phone: (303) 275-4954; Fax: (303) 275-4753
E-mail: jesse.adams@go.doe.gov

Contract Number: DE-FG36-08GO18142

Subcontractor:
Midwest Research Institute, Kansas City, MO

Project Start Date: September 1, 2008
Project End Date: January 31, 2012

Objectives

- Fabricate high-surface-area, multiply surface-functionalized carbon ("substituted materials") for reversible hydrogen storage with superior storage capacity (strong physisorption).
- Characterize materials and storage performance. Evaluate efficacy of surface functionalization, experimentally and computationally, for fabrication of materials with deep potential wells for hydrogen sorption (high binding energies).
- Optimize gravimetric and volumetric storage capacity by optimizing pore architecture and surface composition ("engineered nanospaces").

Technical Barriers

This project addresses the following technical barriers from the Hydrogen Storage section of the Hydrogen, Fuel Cells and Infrastructure Technologies Program Multi-Year Research, Development and Demonstration Plan:

(A) System Weight and Volume
(B) System Cost
(E) Charging/Discharging Rates
(J) Thermal Management
(P) Lack of Understanding of Hydrogen Physisorption and Chemisorption

Technical Targets

This project aims at the development of surface-engineered carbons, made from corncob or other low-cost raw materials, which simultaneously host high surface areas, created in a multi-step process, and a large fraction of surface sites with high binding energies for hydrogen, created by surface functionalization with boron, iron, and lithium. Targets are surface areas in excess of 4,500 m^2/g, average binding energies in excess of 12 kJ/mol, and porosities below 0.8, toward the design of materials that meet the following 2015 DOE hydrogen storage targets:

- Gravimetric storage capacity: 0.055 kg H_2/kg system
- Volumetric storage capacity: 0.040 kg H_2/liter system

Accomplishments

- Manufactured a porous carbon with gravimetric excess adsorption of 0.073 ± 0.003 kg H_2/kg, gravimetric storage capacity of 0.106 ± 0.005 kg H_2/kg carbon (including gas in pore space), and volumetric storage capacity of 0.040 ± 0.002 kg H_2/liter carbon, at 80 K and 50 bar. Validated H_2 uptake measurements by measurements on a standard carbon reference sample, AX-21 MSC-30.
- Analyzed gravimetric excess adsorption isotherms at 80 K on porous carbons in terms of high/low binding energy sites in sub/supra-nm pores, respectively. Found, from Grand Canonical Monte Carlo (GCMC) simulations of adsorbed H_2 in bimodal distributions of such pores, that isotherms up to ~30 bar could successfully be modeled with binding energies of ~9 kJ/mol and ~5 kJ/mol, respectively. The simulations identified significant contributions to the isotherms from multilayers of H_2 in supra-nm pores. Above 30 bar, experimental isotherms were found to rise higher than simulated isotherms, consistent with the presence of binding energies lower than 5 kJ/mol.
- Computed adsorption potentials for boron-substituted graphene from first principles and obtained binding energies (well depths) of 12 kJ/mol for 10 wt% boron. GCMC simulations on the substituted carbon predicted gravimetric and volumetric storage capacities of 0.050 kg H_2/kg

carbon and 0.032 kg H_2/liter carbon, at 298 K and 100 bar.

- Developed analytic relation between gravimetric and volumetric storage capacity, at constant gravimetric excess adsorption. Found that volumetric capacity can be increased significantly, under an insignificant loss of gravimetric capacity, by decreasing the porosity of the adsorbent.

Introduction

High-surface-area carbons from corncob, as developed by our team, show considerable promise for reversible onboard storage of hydrogen at high gravimetric and volumetric storage capacity. A current carbon has a gravimetric storage capacity of 0.11 kg H_2/kg carbon at 80 K and 50 bar. This project is a systematic effort to achieve comparable results at 300 K, by increasing surface areas from currently ~3,000 m^2/g to ~5,000 m^2/g, and substituting carbon with boron and other elements that increase the binding energy for hydrogen. Current high surface areas and high binding energies are hosted by sub-nm pores ("nanopores") created by chemical means. New surface area, created by fission tracks from boron neutron capture, $^{10}B + {}^1n \rightarrow {}^7Li + {}^4He$ (U. Missouri Research Reactor), traversing stacks of graphene sheets, will add as much as another 3,000 m^2/g. Thus boron serves in two functions: (i) raise the binding energy by electron donation from H_2 to electron-deficient B; (ii) provide the platform for creation of additional surface area.

Approach

The approach is an integrated fabrication, characterization, and computational effort. Structural characterization includes determination of surface areas, pore-size distributions, and pore shapes. Storage characterization includes measurements of hydrogen sorption isotherms and isosteric heats. Computational work includes adsorption potentials and simulations of adsorbed films for thermodynamic analysis of experimental isotherms. Comparison of computed and experimental isotherms validates theoretical adsorption potentials and experimental structural data.

Results

Figure 1 shows results for hydrogen excess adsorption on: (i) two porous materials, 3K and 4K, made by us, at 80 K; (ii) a standard carbon reference/calibration sample, AX-21 MSC-30 (courtesy of the National Renewable Energy Laboratory), at 77 K and 80 K; and (iii) carbon sample Anderson AX-21 at 77 K (data from [1, 2]). The results for AX-21 MSC-30 agree within error bars with published data for Maxsorb [3] and exhibit a local maximum at p ~ 40-50 bar, characteristic of high-surface-area, AX-21-type carbons. (On the high-pressure side of the maximum, the density of the nonadsorbed gas grows more rapidly than the density of the adsorbed film.) By contrast, samples 3K and 4K show no such maximum in the pressure range investigated, and their excess adsorption exceeds that of AX-21 and AX-21 MSC-30. Samples 3K and 4K are members of a series of carbons, made from corncob, in which the ratio of potassium hydroxide (KOH) to carbon during chemical activation (treatment at 790°C) was varied from 2:1 ("2K") to 6:1 ("6K"). A systematic analysis was undertaken to understand this unexpected behavior of 3K and 4K. Relevant variables for the analysis are specific surface area, porosity, pore-size distribution, gravimetric storage capacity, and volumetric storage capacity of samples (Figures 1b, c and Table 1). Storage capacity is relevant because it allows us to cross-check computed isotherms (GCMC simulations in bimodal pore-size distributions, Figure 2) for consistency with experimental results for both excess adsorption and storage capacity.

Gravimetric storage capacity, G_{st} (total mass of hydrogen stored, adsorbed film and non-adsorbed gas in pores, per mass of sample), and volumetric storage capacity, V_{st} (total mass of hydrogen stored per volume of sample), were calculated from gravimetric excess adsorption, G_{ex} (mass of excess adsorbed H_2 per mass of sample) using

$$G_{st}(p,T) = G_{ex}(p,T) + [\rho_{gas}(p,T)/\rho_{skel}]\phi/(1-\phi), \quad (1)$$

$$V_{st}(p,T) = G_{ex}(p,T)(1-\phi)\rho_{skel} + \phi\rho_{gas}(p,T), \quad (2)$$

[4], where ϕ, and ρ_{skel} are porosity and skeletal density of the sample, ρ_{gas} is bulk density of H_2 gas, and p, T are pressure and temperature. If volume surrounding the sample, such as in a test bed packed with adsorbent, is included in the pore volume (any surface surrounding a solid, which may or may not include segments of the solid's surface, defines a distinct pore volume) and porosity is evaluated accordingly, Eqs. (1, 2) automatically give the capacities of the bed. It is clear from (1, 2) that G_{st} increases and V_{st} decreases with increasing porosity. Elimination of ϕ from (1, 2) yields

$$V_{st} = \rho_{gas}/[1 - (G_{ex} - \rho_{gas}/\rho_{skel})/G_{st}], \quad (3)$$

which, for any fixed G_{ex}, describes how the volumetric capacity varies with gravimetric capacity (Figure 1c). It also describes the density ratio, V_{st}/ρ_{gas}, between a tank with and without adsorbent. Results (1-3) hold for any gas adsorption system and answer the question, raised by DOE, on how gravimetric and volumetric storage capacity depend on porosity.

The absence of a local maximum in samples 3K and 4K is due to variations in binding energies, and possibly vibrational frequencies of adsorbed H_2 in the

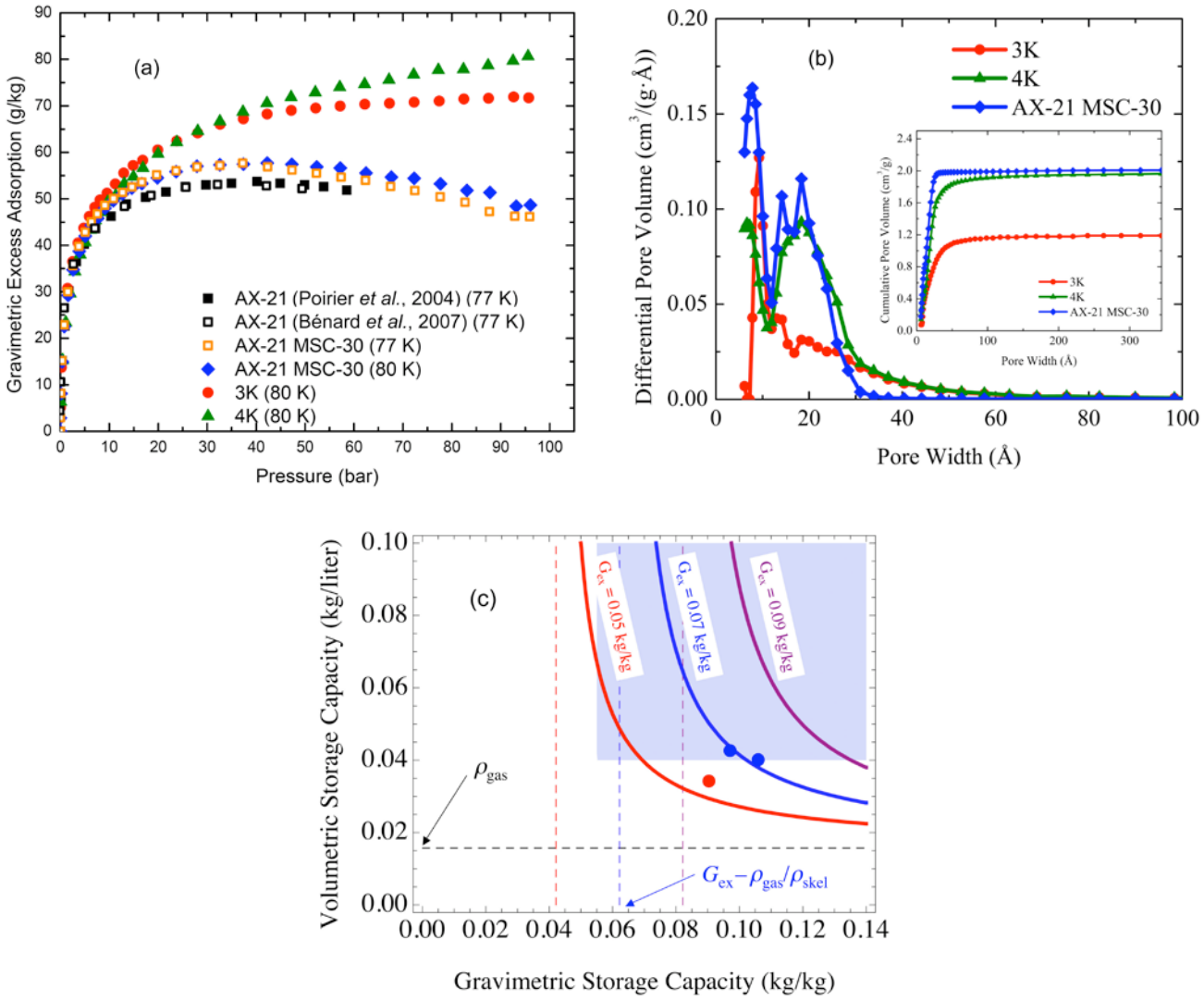

FIGURE 1. (a) Gravimetric excess adsorption isotherms of H_2 on carbon samples 3K, 4K (U. Missouri), and AX-21 MSC-30 (National Renewable Energy Latoratory), all measured on a Hiden HTP1 high-pressure volumetric analyzer (U. Missouri) at indicated temperatures. Also shown are data on carbon sample AX-21 [1, 2]. AX-21 MSC-30 was measured at 77 K for comparison with AX-21, and at 80 K for comparison with samples 3K and 4K. Experimental uncertainties are less than 5%. (b) Differential and cumulative (inset) pore-size distribution of samples AX-21 MSC-30, 3K, and 4K, determined from N_2 adsorption at 77 K and quenched solid-state density functional theory (Quantachrome Autosorb-1-C surface-area analyzer). (c) Gravimetric and volumetric hydrogen storage capacity of samples AX-21 MSC-30, 3K, and 4K, at 80 K and 50 bar (colored dots), from Table 1. The curves are plots of the volumetric vs. gravimetric storage capacity, V_{st} and G_{st}, Eq. (3), at constant gravimetric excess adsorption, G_{ex}, evaluated at 80 K, 50 bar (ρ_{gas} = 0.016 g/cm^3), and ρ_{skel} = 2.0 g/cm^3. Large/small values of G_{st} correspond to high/low porosity at fixed G_{ex}, Eq. (1). So V_{st} rises with decreasing G_{st} because decreasing porosity increases the volumetric storage capacity, Eq. (2). V_{st} nominally diverges when the porosity is nominally zero. The colors of the dots match the color of the nearest value of gravimetric excess adsorption. All storage capacities are material values, not system values. The 2015 DOE gravimetric and volumetric storage system targets are shown as blue area.

adsorption potential [4]. E.g., the steeper rise of excess adsorption at low pressure in sample 3K than in 4K (Figure 1a) indicates that 3K hosts a larger fraction of surface sites with high binding energies (low binding energies make the adsorbed film more compressible, which shifts the maximum of excess adsorption to higher pressures). Likewise, the slower leveling off of excess adsorption at high pressure in 4K than in 3K indicates that 4K hosts a larger fraction of sites with low binding energies. These qualitative conclusions are supported by the data in Figures 1b and 2. Figure 1b shows that the fraction of sub-nm, high-binding-energy pores progressively decreases and the fraction of supra-nm, low-binding-energy pores increases as we go from AX-21 MSC-30 to 3K to 4K. The best fits of simulated excess adsorption isotherms, based on bimodal pore-size distributions, to the experimental data, while less than perfect, confirms this: the nominal fraction of surface

TABLE 1. Hydrogen storage on selected materials. Surface areas, from Brunauer-Emmett-Teller analysis of N_2 adsorption isotherms at 77 K and relative pressures 0.01-0.03, are rounded to the nearest hundred. Porosities were determined from N_2 adsorption at 77 K, at relative pressure 0.995. Gravimetric excess adsorption values are from Figure 1a. Gravimetric and volumetric storage capacities were calculated from Eqs. (1, 2) with $\rho_{skel} = 2.0$ g/cm^3.

	AX-21 MSC-30	3K	4K
Ratio KOH:C for chemical activation	N/A	3:1	4:1
Specific surface area (Σ)	3,400 m^2/g	2,500 m^2/g	2,600 m^2/g
Porosity (ϕ)	0.81	0.78	0.81
Gravim. H_2 excess (G_{ex}; 80 K, 50 bar)	0.057 kg/kg	0.069 kg/kg	0.073 kg/kg
Gravim. H_2 stored (G_{st}; 80 K, 50 bar)	0.090 kg/kg	0.097 kg/kg	0.106 kg/kg
Volum. H_2 stored (V_{st}; 80 K, 50 bar)	0.034 kg/liter	0.043 kg/liter	0.040 kg/liter
Density ratio, V_{st}/ρ_{gas}, (80 K, 50 bar)	2.2	2.7	2.6

sites with binding energy ~9 kJ/mol drops from 65% to 10% to 5% (Figure 2). Best fits of simulations to the low-pressure part of the isotherms only, p ~ 0-30 bar, gave very good agreement with experimental data, both for excess adsorption and storage capacity, with binding energy of ~9 kJ/mol on 20% of surface sites, both for 3K and 4K (not shown). However, above 30 bar, the experimental isotherms were found to exceed the simulated ones. This led to the conclusion that the absence of a local maximum in samples 3K and 4K is due to a significant presence of binding energies *less* than 5 kJ/mol, presumably located at edge sites of fragments of graphitic sheets. The significant fraction of supra-nm pores in 3K and 4K (Figure 1b) is consistent with a significant fraction of such edge sites. The mechanism by which supra-nm pores can give rise to higher excess adsorption than sub-nm pores (Figure 1a), even though binding energies may be low, is multilayer adsorption by attractive H_2-H_2 interactions, effective at low temperature and in wide pores [5], but ineffective in sub-nm pores, too narrow to hold multilayers.

Figure 2 details the high gravimetric storage capacity of samples AX-21 MSC-30, 3K, and 4K at 80 K over the entire pressure range. In Figure 1c, the storage capacities are shown at 50 bar and 80 K and illustrate the nonlinear dependence of volumetric capacity on gravimetric capacity. E.g., the volumetric storage capacity – or, equivalently, the density ratio of adsorbed to compressed H_2, V_{st}/ρ_{gas} ~ 2.5 (Table 1) – could be raised significantly by reducing the porosity, at an insignificant loss of gravimetric storage capacity.

Boron-substituted carbons were made from samples 3K and 4K by sublimation of decaborane ($B_{10}H_{14}$) on the

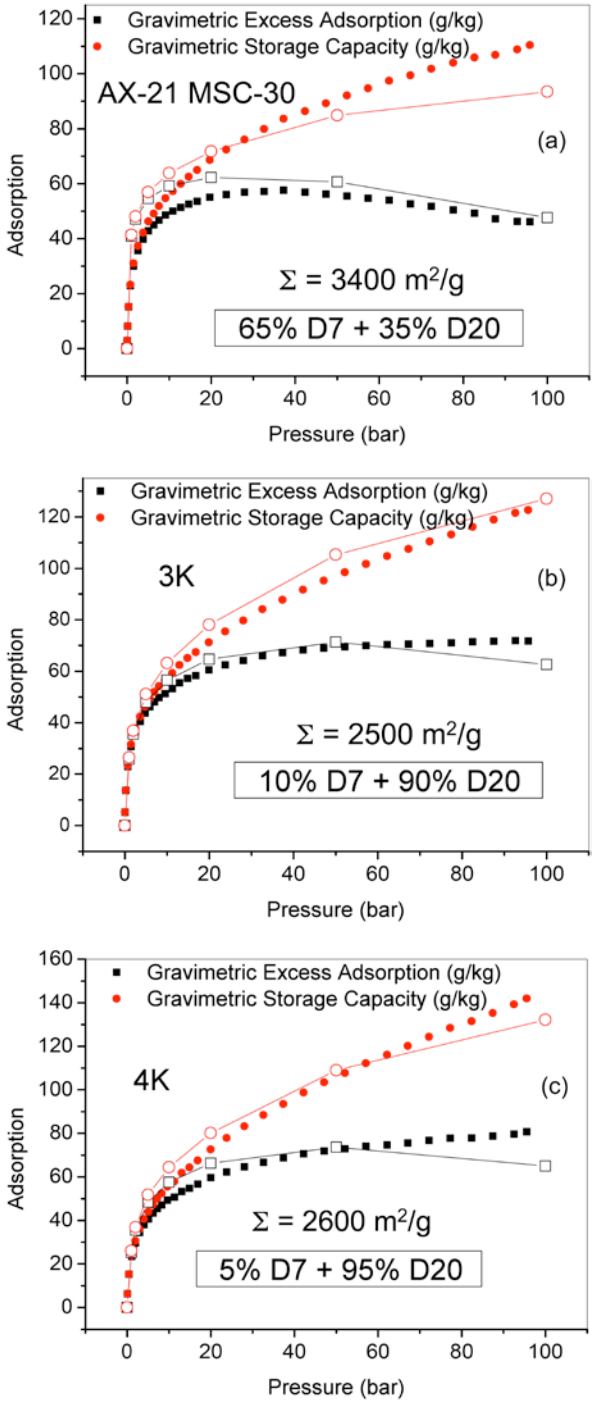

FIGURE 2. Gravimetric excess adsorption and gravimetric storage capacity of H_2 on (a) sample AX-21 MSC-30 at 77 K, (b) sample 3K at 80 K, and (c) sample 4K at 80 K (experimental, full symbols), and GCMC simulations at 77 K (open symbols) on model carbons with a bimodal distribution of slit-shaped pores and specific surface area equal to the experimental area. The slit widths, between centers of carbon atoms on opposite walls, were fixed at 0.7 nm (D7, sub-nm pores, binding energy ~9 kJ/mol) and 2.0 nm (D20, supra-nm pores, binding energy ~5 kJ/mol). The single fitting parameter in each simulation was the fraction of surface area in 0.7 nm pores (the remaining fraction being the surface area in 2.0 nm pores). The fractions reported gave the best fits for excess adsorption over the whole range of pressures.

surface and subsequent thermolysis of the decaborane and annealing. Analyses of surface areas and pore-size distributions before and after substitution demonstrated that boron concentrations up to 10 wt% can be brought into pores of high-surface-area carbons from outside in this way without compromising large surface areas. Investigations of H_2 adsorption on these substituted materials are underway.

To generate systematic models of H_2 storage on boron-substituted carbons as a function of boron concentration and distribution of boron on the surface, we computed adsorption potentials for boron-substituted graphene from first principles and performed GCMC simulations of H_2 adsorption in these potentials. Results are shown in Figure 3 [6]. Boron substitution creates potential wells with binding energy (well depth) of ~5, 8, 9, and 12 kJ/mol for 0, 1, 5, and 10 wt% boron, respectively (Figure 3a, b). The simulations predict gravimetric and volumetric storage capacities of 0.050 kg H_2/kg carbon and 0.032 kg H_2/liter carbon for 10 wt%

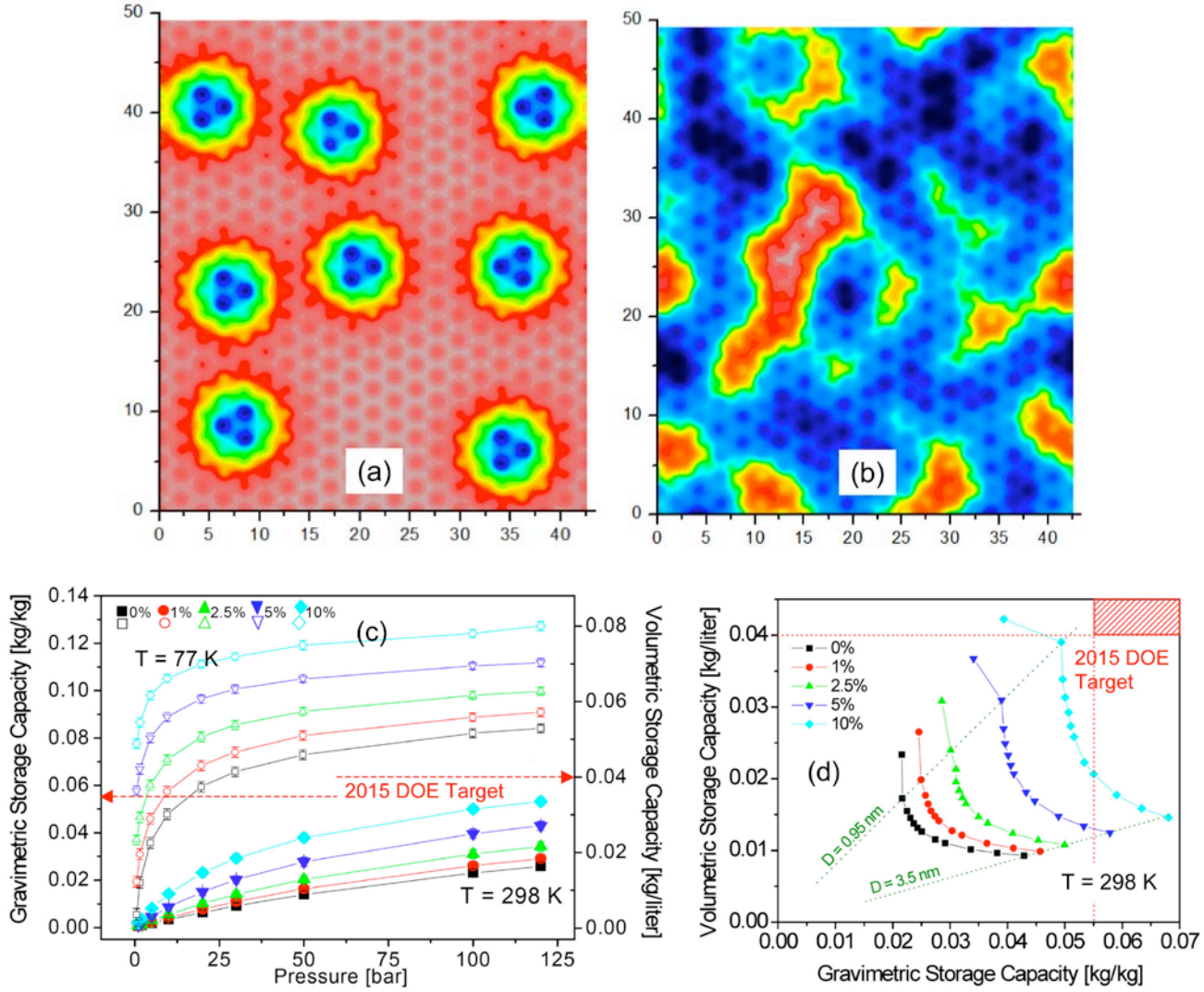

FIGURE 3. Adsorption potentials for H_2 on a boron-substituted graphene sheet containing (a) 1 wt% boron (8 boron atoms), and (b) 5 wt% boron (40 boron atoms). The potentials were computed from second-order Møller-Plesset perturbation theory applied to restricted open-shell Hartree-Fock wave functions. Binding energies range from 5 kJ/mol (pink grey, "carbon") to 9 kJ/mol (dark blue, "boron"). (c) Simulated gravimetric (left axis) and volumetric (right axis) H_2 storage capacities on boron-substituted carbon, with slit-shaped pores of width 1.2 nm, as a function of boron concentration and temperature. (d) Volumetric vs. gravimetric storage capacities of boron-substituted carbons at 298 K and 100 bar, as a function of pore width (different points with same color) and boron concentration (different colors), and in relation to the 2015 DOE volumetric and gravimetric storage system targets. The curves are statistical-mechanical, isoconcentration versions (constant boron concentration) of the curves in Figure 1c. In comparison, the curves in Figure 1c, Eq. (3), are effective-medium, isosteric treatments (constant gravimetric excess adsorption) of volumetric vs. gravimetric storage capacity. The steep rise of V_{st} at low G_{st} here is the analogue of the steep rise of V_{st} in Figure 1c.

boron, 298 K, and 100 bar (Figure 3c). Gravimetric and volumetric storage capacities for variable boron concentration, 298 K, and 100 bar are presented in Figure 3d.

Conclusions and Future Directions

- Assessed that gravimetric excess adsorption isotherms at 80 K on new high-performance carbons, 3K and 4K, unlike AX-21-type carbons, do not exhibit a local maximum in the pressure range 0-100 bar, are significantly higher than excess adsorption of AX-21-type carbons, and give rise to gravimetric and volumetric storage capacities at 80 K and 50 bar which are competitive with those of MOF-177 (~0.10 kg H_2/kg adsorbent).
- Explained this performance in terms of coexistence of binding energies of ~9 kJ/mol in sub-nm pores, of ~5 kJ/mol in supra-nm pores, and of less than 5 kJ/mol on edge sites of locally graphitic sheets, and multilayer adsorption of H_2 in such pore systems.
- Assessed resulting gravimetric and volumetric storage capacities in terms of engineerable gravimetric excess adsorption and porosity (approximately independent design variables).
- Developed roadmap for achievement of comparable storage capacities at room temperature on boron-substituted carbons.
- Future work: study performance of boron-substituted materials as a function of deposition conditions of decaborane and thermal annealing; compare results with other methods of introducing boron; measure isosteric heats of adsorption and compare with results from simulations; study chemical nature of substituted boron by solid-state nuclear magnetic resonance and X-ray photoelectron spectrocsopy.

FY 2009 Publications/Presentations

1. 2009 DOE Hydrogen Program Review, Washington, D.C., May 18-22, 2009. Presentation ST31.

2. L. Firlej, S. Roszak, B. Kuchta, P. Pfeifer, and C. Wexler, "Enhanced Hydrogen Adsorption in Boron Substituted Carbon Nanospaces." Submitted, July, 2009.

3. B. Kuchta, L. Firlej, P. Pfeifer, and C. Wexler, "Numerical Estimation of Hydrogen Storage Limits in Carbon Based Nanospaces." Carbon **47** (2009), doi: 10.1016/j.carbon.2009.09.009.

4. M. Kraus, M. Beckner, J. Burress, J. Ilavsky, C. Wexler, and P. Pfeifer, "Hierarchical Pore Structure Analysis of Engineered Carbon Nanospaces," 5th International Workshop on Characterization of Porous Materials, Rutgers University, New Brunswick, June 24–26, 2009.

5. B. Kuchta, L. Firlej, R. Cepel, P. Pfeifer, and C. Wexler, "Structural and Energetic Factors in Designing a Perfect Nanoporous Sorbent for Hydrogen Storage." 5th International Workshop on Characterization of Porous Materials, Rutgers University, New Brunswick, June 24–26, 2009.

6. M. Beckner, J. Burress, C. Wexler, Z. Yang, F. Hawthorne, and P. Pfeifer, "Boron-Doped Carbon Nanospaces for High-Capacity Hydrogen Storage." 2009 March Meeting of the American Physical Society, Pittsburgh, PA, March 16–20, 2009. Abstract: *Bull. Am. Phys. Soc.* **54**, W27.00010 (2009).

7. J. Burress, M. Beckner, N. Kullman, R. Cepel, C. Wexler, and P. Pfeifer, "Analysis of Hydrogen Adsorption in Engineered Carbon Nanospaces." 2009 March Meeting of the American Physical Society, Pittsburgh, PA, March 16–20, 2009. Abstract: *Bull. Am. Phys. Soc.* **54**, W27.00012 (2009).

8. M. Kraus, M. Beckner, J. Burress, and P. Pfeifer, "Ultra-Small-Angle X-Ray Scattering of Nanoporous Carbons." 2009 March Meeting of the American Physical Society, Pittsburgh, PA, March 16-20, 2009. Abstract: *Bull. Am. Phys. Soc.* **54**, W27.00011 (2009).

9. B. Kuchta, L. Firlej, R. Cepel, P. Pfeifer, and C. Wexler, "Structural and Energetic Factors in Designing a Perfect Nanoporous Sorbent for Hydrogen Storage." 2009 March Meeting of the American Physical Society, Pittsburgh, PA, March 16–20, 2009. Abstract: *Bull. Am. Phys. Soc.* **54**, W27.00014 (2009).

10. J. Romanos, R. Cepel, M. Beckner, M. Kraus, J. Burress, and P. Pfeifer, "Magnetic Properties of High-Surface-Area Carbons and their Effect on Adsorbed Hydrogen." 2009 March Meeting of the American Physical Society, Pittsburgh, PA, March 16-20, 2009. Abstract: *Bull. Am. Phys. Soc.* **54**, W27.00009 (2009).

References

1. E. Poirier *et al.*, *Appl. Phys. A* **78**, 961 (2004).

2. P. Bénard and R. Chahine, *Scr. Mater.* **56**, 803 (2007).

3. W.-C. Xu *et al.*, Int. J. Hydrogen Energy **32**, 2504 (2007).

4. J. Burress *et al.*, Nanotechnol. **20**, 204026 (2009).

5. B. Kuchta *et al.*, *Carbon* **47** (2009), doi: 10.1016/j.carbon.2009.09.009.

6. L. Firlej, S. Roszak, B. Kuchta, P. Pfeifer, and C. Wexler, Submitted (2009).